Advanced Composites and Hybrid Materials (2024) 7:156
https://doi.org/10.1007/s42114-024-00970-y

RESEARCH

Sustainable three-dimensional printing of waste paper-based functional materials and constructs

Chengcheng Cai[1] · Pei Zhang[1] · Yafei Wang[1] · Yun Tan[1] · Iek Man Lei[2,3] · Ben Bin Xu[4] · Ji Liu[1,5]

Received: 5 June 2024 / Revised: 6 September 2024 / Accepted: 17 September 2024 / Published online: 28 September 2024

Abstract

Three-dimensional (3D) printing is a prominent technology across various industrial sectors, and its increasing popularity urgently calls for sustainable 3D printing materials. However, the availability of such materials remains under exploit. Here, we present a low-cost strategy to harnesses waste papers as a feedstock to develop sustainable 3D printing inks. This approach offers a remarkable printability and circular utilisation of biodegradable paper wastes to produce 3D printed constructs, with desired mechanical properties and shape stability for high temperature applications. Our constructs can be efficiently recycled into inks for reprinting, and our method can be applied to various types of waste papers. By employing multi-material printing, our approach can be extended to produce multi-coloured constructs, security information printings, and mechanically appealing designs. This strategy offers an innovative and sustainable solution that addresses the need for repurposing paper wastes, which would otherwise end up in landfills, while concurrently reducing the reliance on virgin plastics for 3D printing.

Keywords 3D printing · Sustainable · Waste paper · Recyclability

1 Introduction

3D printing is offering remarkable flexibility and diversity in material and structure designs, revolutionising a wide variety of industrial sectors, including manufacturing, automotive, medical, and laboratory research [1–5]. As the technology evolves, the increasing demand for 3D printing materials exacerbates the environmental concerns about the materials used [6]. Among 3D printing materials, thermoplastics (e.g. polylactic acid and acrylonitrile butadiene styrene) and light-curable resins are widely used [2]. However, these materials, typically based on non-renewable resources, often exhibit poor degradation rates (Supplementary Table 1) [7–9]. Their production requires high energy demand (> 43 MJ/kg) and results in a high global warming potential (> 2 kg carbon dioxide (CO_2) eq/kg, Fig. 1a and Supplementary Table 2) [10]. In addition, light-curable resins can lead to harmful health effects to users due to the emission of volatile organic compounds (VOCs), to the open air and aquatic ecosystems [11, 12]. While recent advances have established various sustainable and recyclable 3D printing materials, including recyclable thermosetting photopolymers [6, 13–15] and cellulose-based materials [16–19], one drawback lies in the production and recycling processes of recyclable thermosetting photopolymers, which involve inefficient, complex,

Chengcheng Cai and Pei Zhang contributed equally to this work as the first authors.

✉ Iek Man Lei
ieklei@um.edu.mo

✉ Ben Bin Xu
ben.xu@northumbria.ac.uk

✉ Ji Liu
liuj9@sustech.edu.cn

1 Department of Mechanical and Energy Engineering, Southern University of Science and Technology, Shenzhen 518055, China

2 Department of Electromechanical Engineering, University of Macau, Macao 999078, China

3 Centre for Artificial Intelligence and Robotics, University of Macau, Macao 999078, China

4 Mechanical and Construction Engineering, Faculty of Engineering and Environment, Northumbria University, Newcastle Upon Tyne NE1 8, UK

5 Shenzhen Key Laboratory of Intelligent Robotics and Flexible Manufacturing Systems, Southern University of Science and Technology, Shenzhen 518055, China

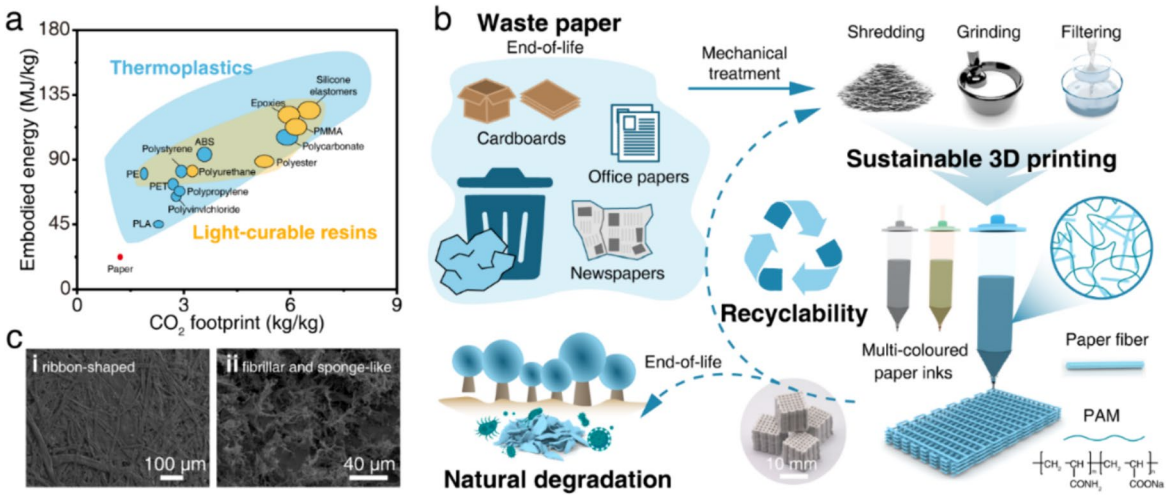

Fig. 1 Waste papers as sustainable 3D printing inks. **a** Plot of embodied energy vs. carbon footprint for the production of conventional plastics. The environmental impact of paper production is provided for reference. Data are compiled from literatures and can be found in Supplementary Table 2. **b** Schematics depicting our strategy of repurposing waste papers into eco-friendly 3D printing inks that enables the creation of recyclable and biodegradable 3D printed constructs. **c** SEM images showing the lignocellulosic fibres of waste office papers before mechanical treatment (i) and the as-prepared paper inks (ii). ABS: acrylonitrile butadiene styrene, PE: polyethylene, PET: polyethylene terephthalate, PLA: polylactic acid, and PMMA: poly (methyl methacrylate)

and costly chemical treatments. Additionally, while numerous studies have depicted the production of 3D printing materials and hydrogels using cellulose microcrystalline, nanocrystal (CNCs), and nanofibers (CNFs) materials with improved printability and stimuli-responsive functionalities, these studies often rely on virgin cellulose feedstocks for production [20–22]. The reliance on virgin resources contradicts the principles of sustainability. It is also worth noting that the current processes to produce nanocellulose, such as CNCs, are highly energy-intensive, time-consuming and require the use of toxic chemicals [23]. Detailed discussion about the limitations of cellulose-based 3D printing can be found in Supplementary Note 1. Therefore, it is highly desirable to explore the possibility of 3D printing using waste materials that are recyclable, degradable, easy to process, and can possess adequate mechanical properties for daily applications. The exploitation of such materials would align with the principles of the 3Rs—reduce, reuse, and recycle.

One promising sustainable, biodegradable, and recyclable choice for 3D printing is waste papers. Derived from renewable lignocellulosic biomass, papers have been integral to our daily lives for over 2000 years [24]. Today, a multitude of paper products has been created for various everyday practices, from documentation to packaging, and the global production of papers reaches nearly 490 million tons by 2023 [25]. However, the current recycling rate of papers is unsatisfactory, contributing around 10–25% of the global landfill waste [26, 27]. The accumulation of paper waste in landfills poses a significant environmental burden. Therefore, with the growing demands for 3D printing materials, repurposing waste papers into printing materials at their end-of-life presents a favourable solution to address both the environmental impact of 3D printing and the paper waste issue.

Here, we present a simple yet economical strategy for repurposing diverse types of waste papers, such as office papers, newspapers, and cardboards, into sustainable direct ink writing (DIW) inks (Fig. 1b). DIW is a widely used 3D printing technique for the eco-friendly processing of sustainable materials [28, 29]. By utilising waste paper fibres to formulate the inks, our inks possess excellent printability and do not require elevated temperature for extrusion. Complex geometrical objects with overhanging designs can be created with ease, while possessing numerous remarkable properties, such as exceptional thermal resistance of up to 200 °C, sufficient mechanical integrity for general use, and the capability to be recycled into 3D printable inks when it reaches the end of its lifespan. Through multi-material printing of different types of paper inks, we demonstrated that multi-coloured constructs, encodable prints for information security, and mechanically appealing biocomposite designs can be realised. Our strategy offers a range of environmental and economic benefits, not only providing waste papers a second life but also paving the way for the sustainable future of 3D printing. In our study, the processing procedures are designed to reduce energy consumption. The printable inks derived from waste paper can be reused for 3D printing, and the 3D-printed constructs can be recycled in subsequent cycles of ink preparation. Furthermore, papers derived from renewable biomass are easily biodegradable, making them

suitable for organic recycling [24]. Thus, the strategy we propose aligns with the principles of the 3Rs—reduce, reuse, and recycle—and supports organic recycling.

2 Results

2.1 Waste papers as sustainable inks for 3D printing

Our strategy is capable of creating printable inks from waste papers that possess the essential rheological properties required for direct ink writing (DIW) (Fig. 1b), a popular and economical extrusion-based 3D printing technique [3, 13]. By formulating paper-based inks that are suitable for DIW, the widespread utilisation of the inks can be enhanced. Supplementary Fig. 1 depicts the ink preparation procedure. We first used waste office papers that are prevalent at home and workplace to exemplify our method. Waste papers are broken down into small fibres using low-cost shredding and grinding methods (Fig. 1b and Supplementary Fig. 1). Subsequently, the paper fibres were mixed with water and passed through a sieve to filter out large particles (> 100 μm). The above mechanical treatments transformed the paper fibres from ribbon-shaped (655 μm in fibre length) to fibrillar and sponge-like morphologies (10.6 μm in fibre length) that are suitable for extrusion (Fig. 1c and Supplementary Fig. 2). Centrifugation was then used to attain a soggy paper pulp composed of lignocellulosic fibres. Finally, a paper ink was obtained by mixing the paper pulp with a small amount (10 w/v%) of polyacrylamide (PAM).

Our paper inks exhibit the requisite rheological characteristics for direct ink writing. Compared with inks composed of only PAM, our paper ink possesses a significantly higher viscosity that favours printability (Fig. 2a). In addition, the ink exhibits a pronounced shear-thinning response. The apparent viscosity decreases sharply by four orders of magnitude (10^4 to 10^0 Pa·s) when the shear rate is increased from 10^{-2} to 10^2 s^{-1}, enabling a smooth extrusion [30]. The low yield stress behaviour of our ink further facilitates the extrusion at modest pressure. Above the yield stress of ~ 3×10^2 Pa, the storage modulus of the ink drops dramatically (Fig. 2b). Our paper ink also exhibits a fast elastic recovery behaviour that promotes shape retention after extrusion. The ink can rapidly recover its storage modulus (> 10^4 Pa) after shearing above its yield stress, indicating its ability to preserve the printed shape for supporting successive layers (Fig. 2c). All of these properties make our ink highly suitable for DIW. PAM serves as a dispersant in our ink formulation to prevent sedimentation of the paper fibres, and its concentration is optimised. The use of 10 w/v% of PAM can significantly prevent ink sedimentation and ensure smooth printing (Supplementary Figs. 3–4). Without PAM, sedimentation of paper fibres occurs, leading to nozzle clogging. To enhance the eco-friendliness of our inks, we have also tested the use of natural dispersants, such as sodium hyaluronate and sodium alginate (Supplementary Figs. 4–5). Similar dispersion effects and printability were observed. Of note, for the rest of the experiments, we mostly used PAM as the dispersant unless otherwise specified.

By leveraging the rheological properties of our paper inks, our ink can be printed layer-by-layer under their own weight with high precision (Supplementary Video 1). Sharp filamentary shape was enabled with no significant spreading marked at the intersection for various infill patterns (i.e. honeycomb, rectilinear, and triangular infills) (Supplementary Fig. 6f and Supplementary Videos 2–3). In addition, through control of the printing setting (e.g. printing rate and extrusion flow rate), only a slight geometry deviation was observed between the computer-aided design (CAD) model and the 3D printed (3DP) model (Supplementary Fig. 6e). To gain further insight into the printability of our paper ink, we fabricated a series of 2D and 3D objects with complex geometric features, such as a spiral ring, a staircase, and an ancient Chinese temple (Fig. 2d). Noteworthily, as explicitly demonstrated in the 3D printed temple, suspended and overhang features with an inclination angle of 45° can be neatly printed, similar to the maximum overhang angle in thermoplastic extrusion-based 3D printing [31]. Moreover, unlike conventional thermoplastics used in extrusion 3D printing (i.e. fused deposition modelling) that require high temperature for extrusion [32], our paper ink can be easily extruded at ambient conditions. The printed features remain stable during a 2-h printing time, indicating the potential for achieving large-scale printing with considerable height using our inks. After printing, the 3D printed constructs were dried by either freeze-drying or ethanol exchange drying methods, resulting in solidified 3D objects.

2.2 Longevity, recyclability, and applicability to a wide range of paper types

The paper constructs have a long service lifetime. We found that the structure of the constructs remains stable, and no sign of micro-organism growth was found over storage of 18 months under ambient temperature and humidity (Supplementary Fig. 7). In addition to the service lifetime, the paper inks exhibit a long shelf-life. The ink maintains its printability after storage for at least 8 months in a sealed bottle (Supplementary Fig. 8). No significant change in the rheological properties was observed, indicating the stable dispersion of paper fibres within our formulated ink (Supplementary Fig. 8a–d).

Circular life cycle is an important aspect towards a sustainable 3D printing practice, given the high failure rate during the 3D printing resulting from incorrect geometry or printer malfunctions [33, 34]. When the constructs reach

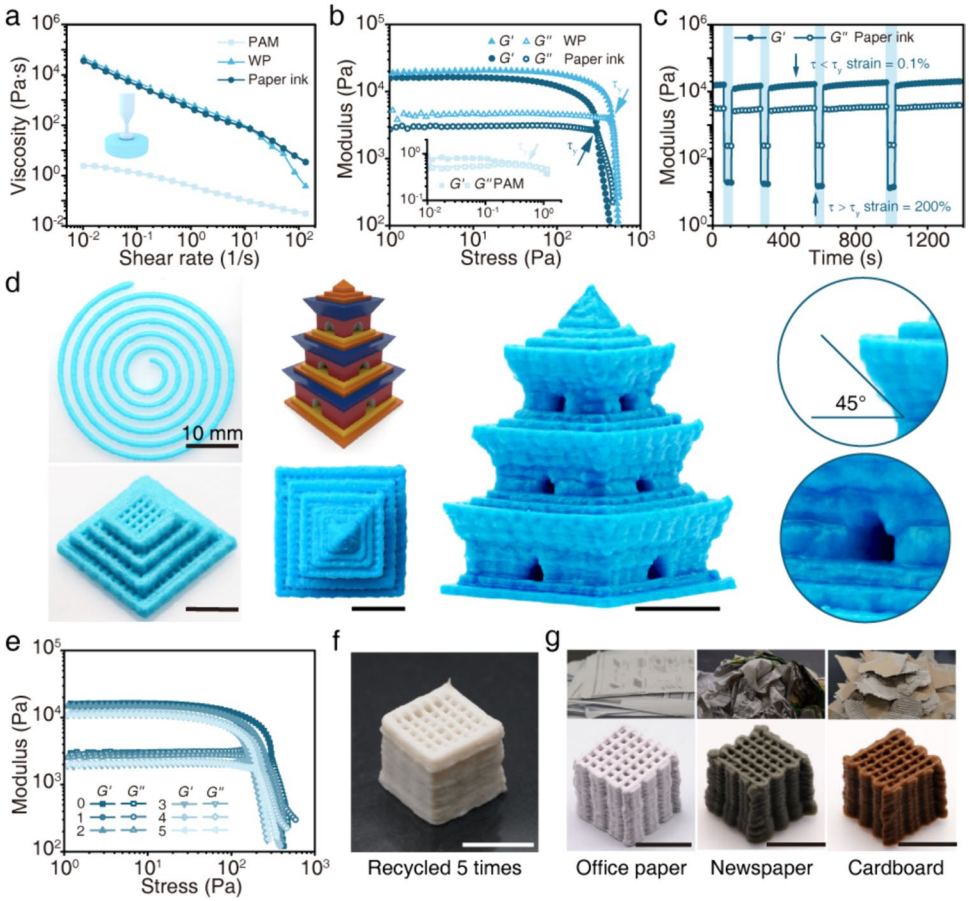

Fig. 2 Printability and shape fidelity of the paper-based inks. **a** Apparent viscosity versus shear rate for the paper ink, the PAM solution (1 wt./vol.%) and the ink composed of paper pulp only without the addition of PAM (waste paper, WP), measured at room temperature. **b** Shear storage modulus (*G'* and *G'')* versus shear stress for the paper ink, the PAM solution and the WP ink. The crossover point (*G'* = *G''*) is taken as the yield stress, indicating the onset of fluidisation. **c** Plots of $G^{'}$ and $G^{''}$ under continuous step-strain measurement between the strain of 0.1% and 200% at a shearing rate of 10 rad/s. **d** Photographs of the 2D and 3D constructs through the 3D printing of our waste paper inks. Scale bar = 10 cm. The paper ink here was stained with a food colouring dye for visualisation. **e** Plots of $G^{'}$ and $G^{''}$ versus shear stress for the office paper inks before (denoted as '0' in the graph) and after five times of recycling. **f** Photograph of the 3D printed (3DP) constructs produced using the paper inks after 5-time recycling treatment. **g** Appearance of the 3DP constructs produced from office papers, newspapers, and cardboards. Scale bar = 1 cm

the end of their useful life or possess printing flaws, our paper-based 3DP constructs can be recycled and processed into printable inks using an approach similar to that used for preparing the virgin inks, where mechanical treatments were used to cleave the printed constructs and lignocellulosic fibres of papers were collected for recycling (Supplementary Fig. 9a). The recycled inks exhibit no observable change in the rheological properties. Similar ink viscosity and storage modulus were attained, despite being recycled for five times (Fig. 2e and Supplementary Fig. 9b). Thus, excellent printability was preserved in the recycled prints (Fig. 2f).

Our protocol can be readily extended to repurpose diverse types of waste papers. In addition to the office papers, we could readily create inks from newspapers and cardboards that inherit their colour characteristics using the same ink preparation method (Fig. 2g). When formulated with the same pulp-to-PAM ratio, these paper inks could be engineered with rheological properties analogous to those of office papers, including storage moduli, shear-thinning properties, and elastic recovery behaviour (Supplementary Figs. 10–11). Therefore, good printability was similarly realised without the need for reoptimizing the printing parameters (Fig. 2g).

2.3 Multi-material printing of coloured and information-encrypted paper constructs

Multi-material printing offers the capability to produce constructs with disparate properties, such as colour and structures. Our office papers inks can be easily stained with dyes owing to the whiteness of office papers. Through multi-material printing of office paper inks dyed with different

colours, we successfully created sophisticated colourful constructs, such as a paper vase (Supplementary Fig. 12 and Supplementary Video 4). This is in contrast to the dark lignin inks developed in previous studies that have colour-tuneability limitations [35, 36]. A wide range of colourful paper inks can be readily crafted for producing attention-grabbing objects.

Further, by harnessing the fluorescent whitening agents present in high-brightness office papers (Supplementary Fig. 13), we created inks with fluorescent and encodable identities as information carriers, analogous to the 'invisible ink' in steganography. Through co-printing this ink with a non-fluorescent paper ink made from tissue papers, we created an encoded motif of the inventor of the papermaking process, 'Cai Lun' (Fig. 3a). The encoded motif was scarcely visible under ambient lighting but decrypted readily under UV light (Fig. 3b). Despite multiple paper inks being involved, no delamination was observed, and the embedded fluorescent pattern remained intact under severe structural deformation, including bending, folding, and rolling (Fig. 3c and Supplementary Video 5). Additionally, the information system can be encrypted, decrypted, and recycled. As an example, we created a QR code with concealed information that is decodable by scanning the code on a smartphone

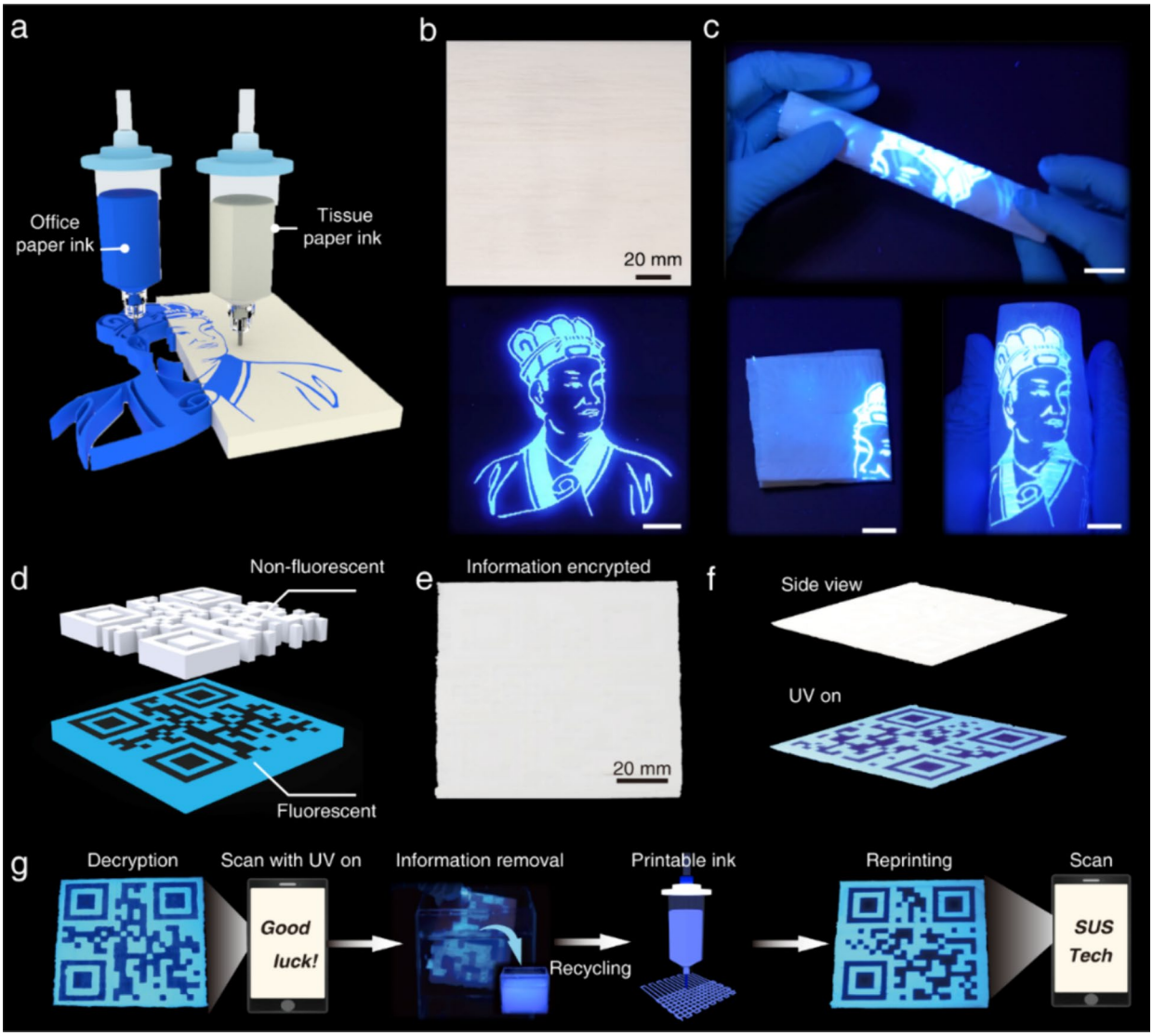

Fig. 3 Multi-material and encrypted 3D printing. **a** Schematic showing the concept of encoded 3D printing with paper inks, which involves the co-printing of a non-fluorescent tissue paper ink and a fluorescent office paper ink. **b** A concealed motif of 'Cai Lun', which could be revealed under ultraviolet (UV) light. **c** Photographs of the 3DP sample under mechanical deformation (e.g. bending, folding and rolling). Scale bars = 20 mm. **d** Schematic of an encrypted 3DP sample with QR code. **e**, **f** The visibility of the QR code under natural light and UV light. **g** Photographs illustrating the decryption, information removal, and recycling of the paper prints for another cycle of encoded 3D printing

under UV light (Fig. 3d–f). Moreover, the 3DP samples can be permanently destroyed and reformulated into another batch of paper inks (Fig. 3g), readily applicable for another cycle of 3D printing of a different information-embedded print (Fig. 3g) or a print for other general purposes. This highlights the potential of our waste paper ink for information encryption and security printing technology.

2.4 Functional paper constructs with stiff and compliant mechanical designs

Next, we explore the mechanical properties of our paper constructs dried by different methods, including freeze-drying, ethanol exchange drying, and air drying, as these properties are crucial in determining their practical applications (Fig. 4a and Supplementary Fig. 14). Our office paper constructs possess specific tensile moduli ranging from 10^{-3} to 10^{-5} GPa/(kg m^{-3}), which is approximately an order of magnitude higher than that of typical elastomeric materials (Fig. 4a). Additionally, their specific strengths range from 10^{-2} to 5×10^{-3} MPa/(kg m^{-3}), approaching the values reported for elastomers (Fig. 4a). The satisfactory structural integrity of the construct is further demonstrated by its load-bearing capability. The 3DP construct that is solidified by freeze-drying can bear a mechanical load of 5000 times heavier than its

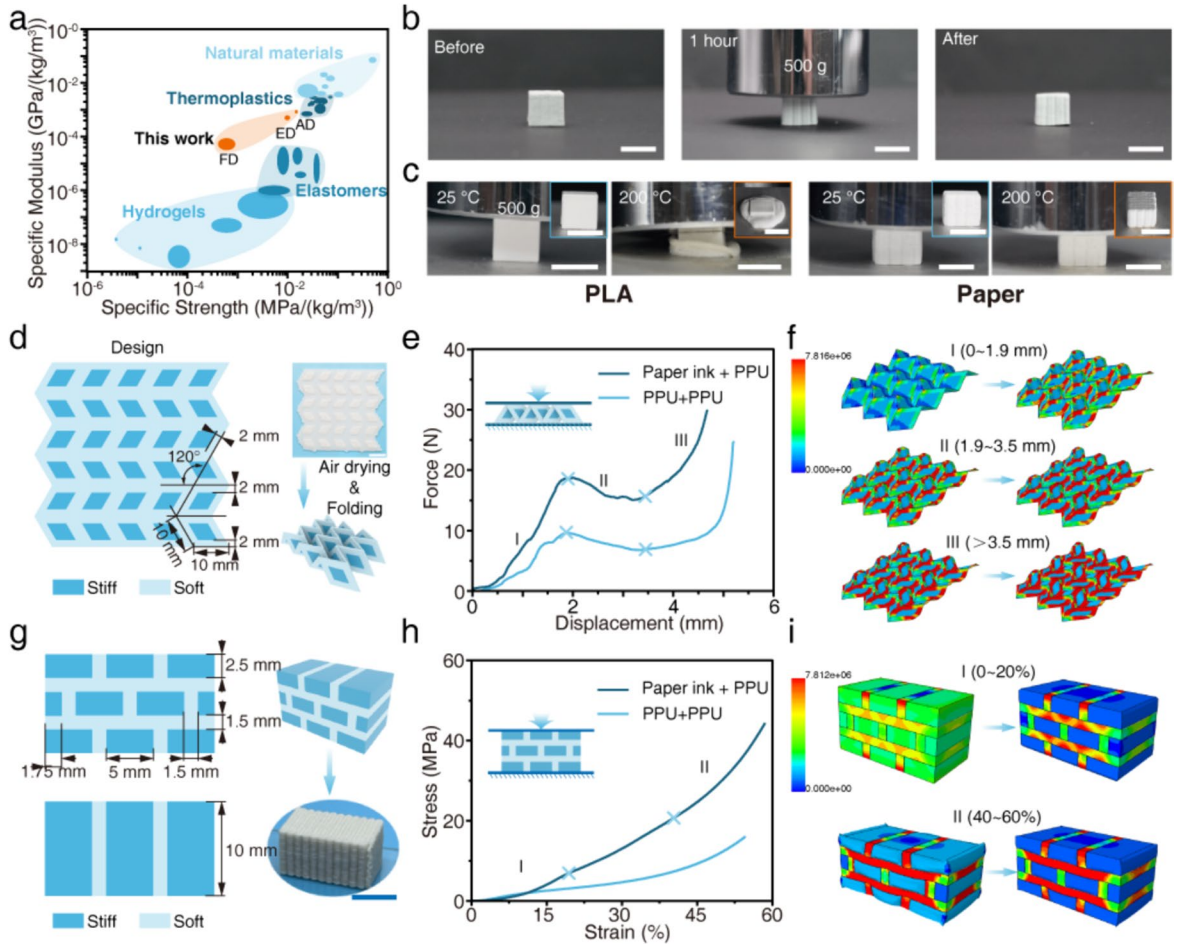

Fig. 4 Mechanical properties of the paper constructs. **a** Chart of specific strength versus specific modulus of various engineering materials and our office paper constructs dried by different methods, including freeze drying (FD), ethanol exchange drying (ED), and air drying (AD). **b** Photographs displaying the load-bearing capability of our freeze-dried paper constructs. Scale bars = 10 mm. **c** Thermal stability of our freeze-dried paper construct and a construct made from PLA. Scale bars = 10 mm. **d** A Miura origami construct composed of stiff and soft domains produced via multi-material printing. The stiff domains were printed using our paper ink, and the soft domains were printed using a composite ink (Paper + polyurethane (PU), referred to as PPU) composed of waterborne polyurethane (PU) and the paper ink. Scale bar = 10 mm. **e** Force-vs-displacement plot of the heterogeneous construct (Paper ink + PPU) and the construct entirely made from the soft ink (PPU + PPU). **f** Stress distribution within the heterogeneous origami construct during a *z*-axis compression obtained from finite element simulation. **g** Heterogeneous tessellated constructs produced. Scale bar = 10 mm. **h** Stress–strain curve of the heterogeneous construct and the construct entirely made from the soft ink. **i** Simulated stress distribution within the heterogeneous tessellated construct under compression

own weight without structural collapsing (Fig. 4b). Constructs made from the recycled inks, the newspaper inks, and the cardboard inks exhibit mechanical properties (i.e. elongation at break, fracture strength, and Young's modulus) of the same order of magnitude (Supplementary Fig. 15–16). Noteworthily, our paper-based constructs possess excellent shape stability at high temperature and can excel in applications that require high-temperature resistance, which overcomes the thermal softening limitation encountered in many 3D printing thermoplastics. After being subjected to a high temperature of 200 °C on a hot plate for 2 h, the structural integrity of the paper constructs experienced no observable change, yet traditional thermoplastics (e.g. polylactic acid and thermoplastic polyurethane) became softened and deformed (Fig. 4c and Supplementary Fig. 17).

Natural structures combining stiff and compliant constituents always demonstrate extraordinary flexibility and strength [37, 38]. While prevalent in natural materials, this integration remains far less explored in engineering structural materials [39, 40]. Thus, exploiting heterogeneous biocomposite designs, such as biomimetic and metamaterial designs, in 3D printing holds great promise for attaining intriguing mechanical behaviours. Our waste paper ink is a desirable eco-friendly candidate for tailoring the mechanical properties of biocomposite constructs [10, 41]. By incorporating waterborne polyurethane, an eco-friendly polymer matrix [42], with our paper ink, a range of stiff-to-compliant mechanical behaviours can be readily attained (Supplementary Fig. 18). Such dissimilar characteristics can be integrated into a single construct by multi-material printing. We created heterogeneous Miura origami and tessellated structures by co-printing a stiff ink composed of the office paper ink and a soft ink composed of the paper ink and PU (Fig. 4d, g and Supplementary Fig. 19). Both heterogeneous constructs, consisting of stiff domains (1150 MPa in Young's modulus) and soft domains (223 MPa in Young's modulus), exhibit a significant reinforcement in mechanical properties. Compared with the homogeneous constructs entirely made with the soft ink, higher fracture strength and higher toughness were observed under compression (Fig. 4e, h). The hard constituents retain the high stiffness, while the soft constituents serve to concentrate the applied stress and provide a means of dissipating strain, as illustrated in our finite element modelling results (Fig. 4f, i, Supplementary Fig. 20, and Supplementary Videos 6–7). This highlights the potential of our waste paper ink for expanding the 3D printing design space towards programmable stiffness designs, creating eco-friendly constructs with reinforced mechanical properties.

3 Conclusion

In summary, we developed a low-cost strategy that utilise waste papers as a feedstock for creating sustainable 3D printing materials, opening a new avenue for sustainable and economical 3D printing. Differing from the existing works on 3D printing cellulose-based materials, our work does not rely on virgin wood or agricultural feedstocks, which might require costly and time-consuming ink preparation. Instead, we make use of waste papers that are cheap and abundant, making our approach highly scalable. Moreover, our approach can easily process waste papers into 3D printing inks using simple and non-toxic solvents. Hence, our inks well align with the sustainability principles of 3Rs.

Our waste paper inks can be printed at ambient temperature, and the resulting paper constructs exhibit remarkable thermal stability of up to 200 °C, which sets them apart from thermoplastics that require high temperature for extrusion and can deform at high temperature (Fig. 5a). Our approach is applicable to a range of waste papers, including those typically considered non-recyclable for paper production, such as tissue papers. Through combining different waste paper inks, potential applications in multi-colour printing, security information printing, and mechanically intriguing designs are enabled. Furthermore, the natural lignocellulosic fibres of our paper constructs offer recyclability and biodegradability potential, providing a sustainable end-of-life solution for 3D prints. This stands in stark contrast to thermoplastics, which can take 10–1000 years to degrade or are even non-degradable (Fig. 5b). Our method is cheaper than other natural materials or materials commonly used in 3D printing as we utilise wastes. Overall, our strategy is not only economical and eco-friendly but also increases the circularity of waste papers and reduces the reliance on virgin plastics.

4 Materials and methods

4.1 Materials

Waste office papers (Deli A4), tissue papers (Vinda gentle facial tissue), newspapers, and cardboards (Express box) were collected in work places and were used directly. Polyacrylamide (PAM, $M_W = 3{,}000{,}000$ Da) was purchased from Sinopharm Chemical Reagent Co., Ltd. (China). Waterborne polyurethane (PU) was purchased from King Chemical Co., Ltd. (China). All chemicals were used without further purification.

4.2 Preparation of waste paper pulps

To prepare printable paper inks, we first created a paper pulp composed of lignocellulosic fibres from waste papers (Supplementary Fig. 1). First, waste papers were cut into small

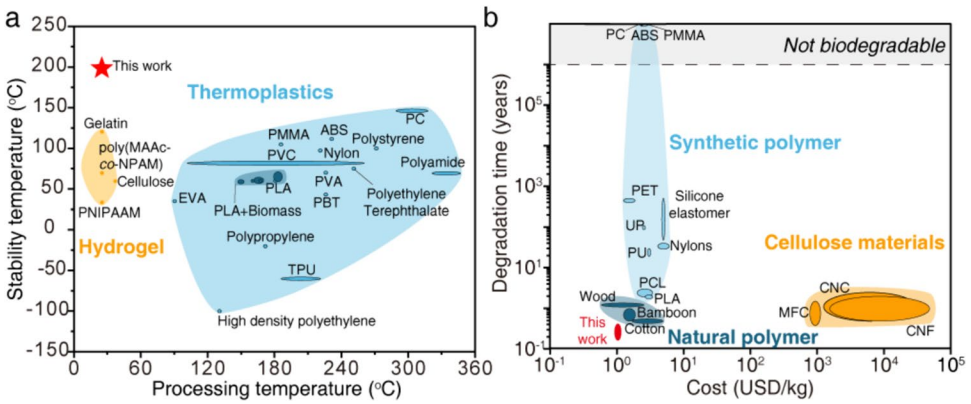

Fig. 5 Comparison of the thermal properties, degradation time, and costs of conventional polymers with our paper constructs. **a** Ashby chart of thermal stability vs. processing temperature and **b** chart of degradation time vs. cost. Data were compiled from literatures that can be found in Supplementary Tables 1 and 6. ABS: acrylonitrile butadiene styrene, EVA: ethylene–vinyl acetate, PBT: polybutylene terephthalate, PC: polycarbonate, PCL: polycaprolactone, PET: polyethylene terephthalate, PLA: polylactic acid, PMMA: poly(methyl methacrylate), PVA: polyvinyl alcohol, PVC: polyvinyl chloride, and TPU: thermoplastic polyurethane

sheets by a paper shredder with a shred width of 4 ~ 5 mm (Deli GA311) and were ground in a mortar grinder (RM 200, Retsch, Germany) with excess water for 3 h. This prolonged grinding time ensures the fibre particles reached the minimal achievable particle size of the grinder. The resulting mixture was resuspended and filtered through a 150-mesh sieve to remove any large paper particles. The suspension was loaded into 50-mL conical tubes and centrifuged at 1000 rpm for 3 min to separate the paper fibers from the solution. The supernatant was then removed, leaving a paper pulp. For every batch of the solution, we measured the paper content of the paper pulp. This involved drying 0.1 g of the paper pulp at 100 °C for 60 min and then weighting the resulting dried pulp to calculate the solid content of the pulp for the following ink preparation. The same protocol was used to create all types of waste paper pulps, including office papers, newspapers, cardboard, and tissue papers used in this study.

4.3 Preparation of 3D printable paper inks

Supplementary Fig. 1 denotes the ink preparation procedure. The waste paper inks were composed of PAM (M_W = 3,000,000 Da), deionised water, and paper fibre in a weight ratio of 0.1:8.9:1, unless otherwise specified. We added paper pulp, which contains water, to the inks. Therefore, the amounts of deionised water and paper pulp added into the inks were determined based on the measured paper content and water content of the paper pulp. All types of paper inks, including office paper, newspaper, cardboard, and tissue paper inks, were prepared using the same formulation ratio.

For the paper filler-reinforced PU inks, two inks were prepared in this study. The ink formulation contains paper fibres, PAM, PU, and water. The water content in both inks is 80% by mass. The remaining 20% is composed of paper fibres, PAM, and PU at mass ratios of 1:0.15:2 and 1:0.15:2, respectively. The amounts of deionised water and paper pulp added were determined based on the paper content and water content of the paper pulps. All inks were homogenised and degassed using a planetary mixer (AR-100, Thinky) at 1000 rpm for 2 min prior to printing. The prepared inks were stored at room temperature in a sealed container when not in use.

4.4 3D Printing of the pulp inks

All 3D printing experiments were conducted using a multi-material direct ink writing printer (3D Bio-Architect WS, Regenovo). The printed structures were designed using a 3D modelling software (Cinema 4D, MAXON) and converted into G-code using a slicing software (Regenovo). Prior to printing, the ink was drawn into a syringe barrel and degassed. The barrel was then loaded into the syringe holder of the printer. A printability test was performed to optimise the printing parameters, including printing speed, extrusion pressure, and nozzle-to-stage distance. The optimised parameters were found to be an extrusion pressure of 100 kPa, a printing speed of 20 mm/s, and a nozzle-to-stage distance of 0.3 mm. All experiments were carried out using nozzles with an outlet diameter of 0.34 mm. All printing was conducted at room temperature. The infill rate varies depending on the model's printing path and spacing. For example, small cubes were printed with an infill rate of approximately 30%, while the origami structures and vases were printed with a 100% infill rate.

4.5 Solidification of the 3DP constructs

After printing, the printed structures were dehydrated and solidified. Three drying methods were tested in this study, including freeze-drying, air-drying, and ethanol exchange drying. Unless otherwise noted, all 3D structures were freeze-dried, and all 2D prints were air-dried. For freeze-drying, the 3D constructs were placed in a refrigerator at − 20 °C for 12 h to ensure they were frozen prior to loading them to a freeze-dryer (Scientz, China). The constructs were then freeze-dried at − 80 °C under a pressure of 1 Pa for 12 h. For air-drying, the 2D prints were left at ambient conditions until fully dried, which took 4–12 h in this study, depending on the size of the print. Samples dried via ethanol exchange drying were also prepared for mechanical tests. For ethanol exchange drying, the constructs were transferred to an anhydrous ethanol solution and soaked for 12 h. The constructs were then dried at ambient temperature on a sieve that enables ease of removal after drying. We noted that shrinkage of the 3D printed constructs happened with the ethanol exchange drying method. To precisely preserve the designated shape, a scale factor of 2.8 was applied to the print model for shrinkage compensation.

4.6 Construct recycling

To recycle the printed constructs, a process similar to the paper ink preparation was adopted. This process involved mechanical shredding, grinding, filtration, and centrifugation to obtain a pulp precipitate. The yield of the lignocellulosic paper fibre was around 98% for each recycling cycle. The resulting paper pulp was then mixed with PAM in a mass ratio of 10:1 to obtain a recycled paper ink. The printed samples created using the recycled paper ink were then air-dried at room temperature and subsequently subjected to mechanical testing.

4.7 Finite element modelling

All numerical simulations in this work were carried out using a commercial finite-element software, ABAQUS (Version 2022, SIMULIA, France). Two finite element models, the Miura-origami model and tessellated model, were developed to simulate the stress distribution or strain distribution within the models under z-axis compression. The models, consisting of stiff domains and soft domains, were built according to the geometrical dimensions stated in Fig. 4d, g, with the thickness of the Miura-origami model as 2 mm. The experimentally measured stress–strain curves and Poisson's ratio of the soft domains (paper ink mixed with PU) and the hard domains (paper ink) were imported as the material parameters of the respective domains for further simulation.

For simulation of the Miura-origami model, an implicit dynamic analysis was adopted where a slow loading (1 mm/min) was employed to emulate the quasi-static compression used in the experiments. For simulation of the tessellated model, a non-linear static finite element simulation was adopted which activating nonlinear configurations. A compression speed along the z-direction was set as 1 mm/min which was applied to the top surface of the model. A mesh convergence test was conducted to obtain an optimal mesh size for accurate simulation results at an acceptable simulation time.

4.8 Optical microscope observation

Optical microscope (DM 2700 M, Leica, Germany) was used to visualise the paper fibre length before and after grinding. The fibres in the pulp were dispersed in water and a dried droplet of the dispersion was observed using the microscope.

4.9 Scanning electron microscopy

Before carrying out imaging using a field-emission SEM (Merlin, Zeiss), the samples were fractured under liquid nitrogen and sputtered with platinum using a sputter coater (Q150TES, Quorum). SEM was performed at an acceleration voltage of 5 kV and an electric current of 100 pA.

4.10 Fibre length statistics

To evaluate the distribution of length of the paper fibres before and after the mechanical treatments, 0.01 g of paper pulp was dispersed in 5 mL of water. The solution was placed in an ultrasonic bath for 20 min to ensure proper dispersion, and then, a droplet of the solution was placed on a dust-free glass slide and allowed to dry under ambient air. Micrographs of the samples were taken using an optical microscope. The length of the fibres in the micrographs were measured using ImageJ software (Version 1.54 h). The number of fibres in each group of samples is $n > 500$.

4.11 Confocal microscopy

To evaluate the geometry deviation between the computer-aided design (CAD) model and the 3D printed model, a staircase sample (dimensions: 5.5 mm in height, 10 mm in length, and 10 mm in width) was fabricated using a paper ink, and its dimensions were acquired using a laser scanning confocal microscope (VK-X1000, Keyence).

4.12 Rheometry

All rheological measurements were carried out using a rheometer (DHR rheometer, TA instruments) equipped with a parallel-plate geometry (20 mm in diameter) at room temperature, and a gap size of 1000 μm was used. Shear viscosity measurements were performed in a steady-state flow mode over a shear rate range of 0.01–500 s^{-1}. Dynamic oscillatory strain amplitude sweep measurements were conducted at a frequency of 10 rad/s in an amplitude range of 0.01–200%. Oscillatory thixotropy and rotational thixotropy tests were also performed to determine the time-dependent moduli and viscosity recovery behaviours of the inks. In oscillatory thixotropy tests, an altered shear rate was applied stepwise between 0.1 and 200%, while in rotational thixotropy tests, an altered shear stress was applied between 0.1 and 200%. The results were analysed using TA Instruments TRIOS software.

4.13 Mechanical testing

All tensile tests were conducted using a universal testing machine (CMT2000K, SANSI, China) equipped with a 500 N load cell. Samples (10 mm × 10 mm × 0.2 mm) were clamped between two grippers and were tested at deformation rates of 1 mm min^{-1} (waste paper samples) and 20 mm min^{-1} (pure PU) at room temperature. Compression tests were conducted using an electronic universal testing machine (MTS, 100 kN load cell, USA) at a deformation rate of 1 mm min^{-1}.

4.14 Photograph and video recording

Unless otherwise specified, all photographs in this work were taken with a SONY camera (A7RIV, Japan), and all videos were recorded using a Nikon camera (D7500, Japan).

4.15 Statistical analysis

All the results in this study were presented as mean ± S.D., and all the mechanical properties presented in this study were measured from at least three parallel samples. Data distribution was assumed to be normal for all the parametric tests, but not formally tested, and no significant difference analysis was performed. The statistical analyses were carried out with the OriginPro 2021 software.

Supplementary Information The online version contains supplementary material available at https://doi.org/10.1007/s42114-024-00970-y.

Author contribution Chengcheng Cai, Pei Zhang, Iek Man Lei, Ben Bin Xu, and Ji Liu wrote the main manuscript text. Chengcheng Cai and Pei Zhang conducted all experiments. Yafei Wang, Ben Bin Xu, and Yun Tan performed numerical simulation and analysis. Chengcheng Cai, Pei Zhang, and Ji Liu conceived the idea and designed the research. All authors reviewed the manuscript.

Funding This study was supported by the National Natural Science Foundation of China (52373139), Natural Science Foundation of Guangdong Province (2022A1515010152 and 2023A1515110532), Basic Research Program of Shenzhen (20231116101626002), and Scientific Research Platforms and Projects of University of Guangdong Provincial Education Office (2022ZDZX3019). This work was also supported in part by the Science, Technology and Innovation Commission of Shenzhen Municipality (ZDSYS20220527171403009). I.M.L. acknowledges the funding support from the Science and Technology Development Fund, Macau SAR (0119/2022/A3 and 0009/2023/ITP1) and the Research Grant from the University of Macau and the University of Macau Development Foundation (SRG2022-00038-FST and MYRG-GRG2023-00225-FST-UMDF). B. B. X. is grateful for the support from the Engineering and Physical Sciences Research Council (EPSRC, UK) grant-EP/N007921.

Data availability No datasets were generated or analysed during the current study.

Declarations

Competing interests The authors declare no competing interests.

References

1. Capel AJ, Rimington RP, Lewis MP, Christie SDR (2018) 3D printing for chemical, pharmaceutical and biological applications. Nat Rev Chem 2(12):422–436. https://doi.org/10.1038/s41570-018-0058-y
2. Truby RL, Lewis JA (2016) Printing soft matter in three dimensions. Nature. 540(7633):371–378 https://doi.org/10.1038/nature21003
3. Skylar-Scott MA, Mueller J, Visser CW, Lewis JA (2019) Voxelated soft matter via multimaterial multinozzle 3D printing. Nature 575(7782):330–335. https://doi.org/10.1038/s41586-019-1736-8
4. Choong YYC, Tan HW, Patel DC, Choong WTN, Chen CH, Low HY, Tan MJ, Patel CD, Chua CK (2020) The global rise of 3D printing during the COVID-19 pandemic. Nat Rev Mater 5(9):637–639. https://doi.org/10.1038/s41578-020-00234-3
5. Wang F, Xue Y, Chen X, Zhang P, Shan L, Duan Q, Xing J, Lan Y, Lu B, Liu J (2023) 3D printed implantable hydrogel bioelectronics for electrophysiological monitoring and electrical modulation. Adv Funct Mater 34(21). https://doi.org/10.1002/adfm.202314471
6. Zhang B, Kowsari K, Serjouei A, Dunn ML, Ge Q (2018) Reprocessable thermosets for sustainable three-dimensional

printing. Nat Commun 9(1):1831. https://doi.org/10.1038/s41467-018-04292-8
7. Mohanty AK, Wu F, Mincheva R, Hakkarainen M, Raquez J-M, Mielewski DF, Narayan R, Netravali AN, Misra M (2022) Sustainable polymers. Nat Rev Methods Primers 2(1). https://doi.org/10.1038/s43586-022-00124-8
8. Guan QF, Yang HB, Han ZM, Ling ZC, Yu SH (2020) An all-natural bioinspired structural material for plastic replacement. Nat Commun 11(1):5401. https://doi.org/10.1038/s41467-020-19174-1
9. Rosenboom JG, Langer R, Traverso G (2022) Bioplastics for a circular economy. Nat Rev Mater 7(2):117–137. https://doi.org/10.1038/s41578-021-00407-8
10. Oliaei E, Olsen P, Lindstrom T, Berglund LA (2022) Highly reinforced and degradable lignocellulose biocomposites by polymerization of new polyester oligomers. Nat Commun 13(1):5666. https://doi.org/10.1038/s41467-022-33283-z
11. Oskui SM, Diamante G, Liao C, Shi W, Gan J, Schlenk D, Grover WH (2015) Assessing and reducing the toxicity of 3D-printed parts. Environ Sci Technol Lett 3(1):1–6. https://doi.org/10.1021/acs.estlett.5b00249
12. Stefaniak AB, Bowers LN, Knepp AK, Luxton TP, Peloquin DM, Baumann EJ, Ham JE, Wells JR, Johnson AR, LeBouf RF, Su FC, Martin SB, Virji MA (2019) Particle and vapor emissions from vat polymerization desktop-scale 3-dimensional printers. J Occup Environ Hyg 16(8):519–531. https://doi.org/10.1080/15459624.2019.1612068
13. Liu Z, Fang Z, Zheng N, Yang K, Sun Z, Li S, Li W, Wu J, Xie T (2023) Chemical upcycling of commodity thermoset polyurethane foams towards high-performance 3D photo-printing resins. Nat Chem 15(12):1773–1779. https://doi.org/10.1038/s41557-023-01308-9
14. Lopez de Pariza X, Varela O, Catt SO, Long TE, Blasco E, Sardon H (2023) Recyclable photoresins for light-mediated additive manufacturing towards Loop 3D printing. Nat Commun 14(1):5504. https://doi.org/10.1038/s41467-023-41267-w
15. Cui J, Liu F, Lu Z, Feng S, Liang C, Sun Y, Cui J, Zhang B (2023) Repeatedly recyclable 3D printing catalyst-free dynamic thermosetting photopolymers. Adv Mater 35(20):e2211417. https://doi.org/10.1002/adma.202211417
16. Siqueira G, Kokkinis D, Libanori R, Hausmann MK, Gladman AS, Neels A, Tingaut P, Zimmermann T, Lewis JA, Studart AR (2017) Cellulose nanocrystal inks for 3D printing of textured cellular architectures. Adv Funct Mater 27(12). https://doi.org/10.1002/adfm.201604619
17. Wang J, Chiappone A, Roppolo I, Shao F, Fantino E, Lorusso M, Rentsch D, Dietliker K, Pirri CF, Grutzmacher H (2018) All-in-one cellulose nanocrystals for 3D printing of nanocomposite hydrogels. Angew Chem Int Ed Engl 57(9):2353–2356. https://doi.org/10.1002/anie.201710951
18. Hausmann MK, Siqueira G, Libanori R, Kokkinis D, Neels A, Zimmermann T, Studart AR (2019) Complex-shaped cellulose composites made by wet densification of 3D printed scaffolds. Adv Funct Mater 30(4). https://doi.org/10.1002/adfm.201904127
19. Thakur MSH, Shi C, Kearney LT, Saadi MASR, Meyer MD, Naskar AK, Ajayan PM, Rahman MM (2024) Three-dimensional printing of wood. Sci Adv 10(11). https://doi.org/10.1126/sciadv.adk3250
20. Clarkson CM, El Awad Azrak SM, Forti ES, Schueneman GT, Moon RJ, Youngblood JP (2021) Recent developments in cellulose nanomaterial composites. Adv Mater 33(28):e2000718. https://doi.org/10.1002/adma.202000718
21. Cao D, Xing Y, Tantratian K, Wang X, Ma Y, Mukhopadhyay A, Cheng Z, Zhang Q, Jiao Y, Chen L, Zhu H (2019) 3D printed high-performance lithium metal microbatteries enabled by nanocellulose. Adv Mater 31(14):e1807313. https://doi.org/10.1002/adma.201807313
22. Zhu P, Yu Z, Sun H, Zheng D, Zheng Y, Qian Y, Wei Y, Lee J, Srebnik S, Chen W, Chen G, Jiang F (2024) 3D printed cellulose nanofiber aerogel scaffold with hierarchical porous structures for fast solar-driven atmospheric water harvesting. Adv Mater 36(1):e2306653. https://doi.org/10.1002/adma.202306653
23. Trache D, Tarchoun AF, Derradji M, Hamidon TS, Masruchin N, Brosse N, Hussin MH (2020) Nanocellulose: from fundamentals to advanced applications. Front Chem 8:392. https://doi.org/10.3389/fchem.2020.00392
24. Hubbe M, Bowden C (2009) Handmade paper: a review of its history, craft, and science. BioResources 4(4):1736–1792. https://doi.org/10.15376/biores.4.4.1736-1792
25. Yang M, Li J, Wang S, Zhao F, Zhang C, Zhang C, Han S (2023) Status and trends of enzyme cocktails for efficient and ecological production in the pulp and paper industry. J Clean Prod 418. https://doi.org/10.1016/j.jclepro.2023.138196
26. Sharma KD, Jain S (2020) Municipal solid waste generation, composition, and management: the global scenario. Soc Responsib J 16(6):917–948. https://doi.org/10.1108/srj-06-2019-0210
27. Laurijssen J, Marsidi M, Westenbroek A, Worrell E, Faaij A (2010) Paper and biomass for energy?: The impact of paper recycling on energy and CO_2 emissions. Resour, Conserv Recycl 54(12):1208–1218. https://doi.org/10.1016/j.resconrec.2010.03.016
28. Haque ANMA, Naebe M, Mielewski D, Kiziltas A (2023) Waste wool/polycaprolactone filament towards sustainable use in 3D printing. J Clean Prod 386. https://doi.org/10.1016/j.jclepro.2022.135781
29. Arif ZU, Khalid MY, Noroozi R, Hossain M, Shi HH, Tariq A, Ramakrishna S, Umer R (2023) Additive manufacturing of sustainable biomaterials for biomedical applications. Asian J Pharm Sci 18(3). https://doi.org/10.1016/j.ajps.2023.100812
30. Cooke ME, Rosenzweig DH (2021) The rheology of direct and suspended extrusion bioprinting. APL Bioeng 5(1):011502. https://doi.org/10.1063/5.0031475
31. Fu Y-F, Rolfe B, Chiu LNS, Wang Y, Huang X, Ghabraie K (2019) Design and experimental validation of self-supporting topologies for additive manufacturing. Virtual Phys Prototyp 14(4):382–394. https://doi.org/10.1080/17452759.2019.1637023
32. Hartings MR, Ahmed Z (2019) Chemistry from 3D printed objects. Nat Rev Chem 3(5):305–314. https://doi.org/10.1038/s41570-019-0097-z
33. Brion DAJ, Pattinson SW (2022) Generalisable 3D printing error detection and correction via multi-head neural networks. Nat Commun 13(1):4654. https://doi.org/10.1038/s41467-022-31985-y
34. Voet VSD, Guit J, Loos K (2021) Sustainable photopolymers in 3D printing: a review on biobased, biodegradable, and recyclable alternatives. Macromol Rapid Commun 42(3):e2000475. https://doi.org/10.1002/marc.202000475
35. Nguyen NA, Barnes SH, Bowland CC, Meek KM, Littrell KC, Keum JK, Naskar AK (2018) A path for lignin valorization via additive manufacturing of high-performance sustainable composites with enhanced 3D printability. Sci Adv 4(12):eaat4967. https://doi.org/10.1126/sciadv.aat4967
36. Kaschuk JJ, Al Haj Y, Rojas OJ, Miettunen K, Abitbol T, Vapaavuori J (2022) Plant-based structures as an opportunity to engineer optical functions in next-generation light management. Adv Mater 34(6):e2104473. https://doi.org/10.1002/adma.202104473
37. Wegst UG, Bai H, Saiz E, Tomsia AP, Ritchie RO (2015) Bioinspired structural materials. Nat Mater 14(1):23–36. https://doi.org/10.1038/nmat4089
38. Nepal D, Kang S, Adstedt KM, Kanhaiya K, Bockstaller MR, Brinson LC, Buehler MJ, Coveney PV, Dayal K, El-Awady JA, Henderson LC, Kaplan DL, Keten S, Kotov NA, Schatz GC,

Vignolini S, Vollrath F, Wang Y, Yakobson BI, Tsukruk VV, Heinz H (2023) Hierarchically structured bioinspired nanocomposites. Nat Mater 22(1):18–35. https://doi.org/10.1038/s41563-022-01384-1
39. Libanori R, Erb RM, Reiser A, Le Ferrand H, Suess MJ, Spolenak R, Studart AR (2012) Stretchable heterogeneous composites with extreme mechanical gradients. Nat Commun 3:1265. https://doi.org/10.1038/ncomms2281
40. Liu X, Wu J, Qiao K, Liu G, Wang Z, Lu T, Suo Z, Hu J (2022) Topoarchitected polymer networks expand the space of material properties. Nat Commun 13(1):1622. https://doi.org/10.1038/s41467-022-29245-0
41. Mohanty AK, Vivekanandhan S, Pin JM, Misra M (2018) Composites from renewable and sustainable resources: challenges and innovations. Science 362(6414):536–542. https://doi.org/10.1126/science.aat9072
42. Kang SY, Ji Z, Tseng LF, Turner SA, Villanueva DA, Johnson R, Albano A, Langer R (2018) Design and synthesis of waterborne polyurethanes. Adv Mater 30(18):e1706237. https://doi.org/10.1002/adma.201706237